Scientific paper

Micellar Properties of Nonionic Surfactant Tween 40® in Water: Small-Angle X-Ray Scattering Study†

Marija Bešter-Rogač

Faculty of Chemistry and Chemical Technology, University of Ljubljana, SI-1000 Ljubljana, Slovenia.

** Corresponding author: E-mail: marija.bester@fkkt.uni-lj.si*

Received: 25-05-2007

†Dedicated to Prof. Dr. Jože Škerjanc on the occasion of his 70th birthday

Abstract

The structural properties of a nonionic surfactant polyoxyethylenesorbitan monopalmitate ($C_{62}H_{122}O_{26}$, commercial names Tween 40®, Polysorbate 40) in aqueous solutions in the temperature range between 15 and 45 °C have been studied by small-angle X-ray scattering (SAXS) technique. Low concentration experimental data were evaluated using the model free indirect Fourier transformation method (IFT), whereas at higher concentration a generalized indirect Fourier transformation method (GIFT) based on the simultaneous determination of intra- and interparticle scattering contributions was applied. It was found that in Tween 40® aqueous solutions globular micelles with maximum distance within one particle of about 9 nm and radii of the hydrophobic core between 2.1–2.4 nm are present. The concentration and the temperature do affect neither the size nor the shape of the micelles considerably, however the presence of the non-spherical and/or elongated aggregates at higher concentrations at all temperatures could be assumed.

Keywords: Tween 40®, water solutions, small-angle X-ray scattering, structural investigation

1. Introduction

Although microemulsions have been known for a long time, there are only few commercial products based on them. Recently, an astonishing statment could be read[1] that there are no food products based on microemulsions. One of the reasons that prevent the incorporation of these systems in foods has been ascribed to the lack of sufficient food-grade types of surfactants that can form large isotropic regions. In this aspect, Tweens (ethoxylated derivates of sorbitan esters) are an interesting family of surfactant. The ability of Tweens to form microemulsions for pharmaceutical[2,3,4,5] and food products[6,7] applications has been studied by few authors. Recently, a pharmaceutically usable microemulsion system prepared from water, isopropyl myristate with Tween 40®, and Imwitor 308® as possible drug delivery system has been investigated thoroughly in our laboratories.[8,9,10]

Tween 40® (polyoxyethylenesorbitan monopalmitate, Polysorbate 40) is a strongly hydrophilic surface active agent. It is used as an emulsifier, often in combination with sorbitan esters, and its structure (Scheme 1) also enables it to fulfil other functions, such as the modification of fat crystallization.[11] Within the European Union it is labelled as a food additive with the number E 434[12] and is permitted in food (in fat emulsions for baking purposes, desserts, ice-cream, sugar confectionery, emulsified sauces, soups, dietary food supplements, chewing gum etc.) and in non-food applications (cosmetics, animal feed, plastic industry).

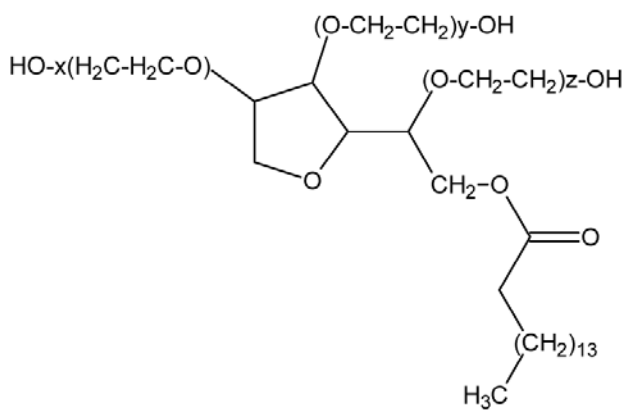

Scheme 1: Schematic representation of a nonionic surfactant Tween 40® (the total number of oxyethylene units: x + y + z = 20).

Although a considerable number of papers on microemulsion systems involving Tweens have appeared in the literature, there are only few systematic studies on their micellar properties in aqueous solution,[13] mixed solvents[14,15,16] or in the binary and ternary surfactant mixtures.[17,18,19] However, there is no structural investigation on these systems which could contribute to better understanding of the structure-function relationship.

In order to obtain a more complete understanding of the micellar properties of Tween 40® in aqueous solution we have studied the effect of the concentration and temperature on the size, shape, internal structure and interparticle interactions in solution by small-angle X-ray scattering (SAXS) technique.

2. Materials and Methods

2. 1. Materials

The surfactant Tween 40® was purchased from Fluka (Chemie GmbH, Switzerland) and used as received. Solutions were prepared by weighing of the surfactant and triple distilled water and were stored at room temperature in plastic sample holder.

2. 2. Small Angle X-ray Scattering (SAXS)

SAXS measurements were performed with an evacuated Kratky compact camera system (Anton Paar, Graz, Austria) with a block collimating unit, attached to a conventional X-ray generator (Bruker AXS, Karlsruhe, Germany) equipped with a sealed X-ray tube (Cu-anode target type) producing Ni-filtered Cu K_α X-rays with a wavelength of 0.154 nm. The tube was operating at 35 kV and 35 mA. The samples were transferred to a standard quartz capillary placed in a thermally controlled sample holder centered in the X-ray beam. The scattering intensities were measured with a linear position sensitive detector (PSD 50m, M. Braun, Garsching, Germany) detecting the scattering pattern within the whole scattering range simultaneously. Measurements were performed at 15, 25, 35 and 45 °C. For each sample, five SAXS curves with a sampling time of 15000 seconds were recorded and subsequently averaged to ensure reliable statistics, smoothed, and corrected for solvent scattering. The absorption of the solutions was determined by using the 'moving slit' method.[20]

The smeared data were corrected for experimental broadening by numerical de-smearing based on the measured beam cross-section profiles. The result of these calculations is a desmeared scattering function and the pair-distance distribution function $p(r)$:

$$p(r) = \frac{1}{2\pi^2}\int_0^\infty I(q)(qr)\sin(qr)dq\,, \qquad (1)$$

which is the Fourier transform of the scattering function:[21]

$$I(q) = 4\pi\int_0^\infty p(r)\frac{\sin(qr)}{qr}dr\,, \qquad (2)$$

where q is a scattering vector defined as $q = (4\pi/\lambda)\sin(\theta/2)$, λ is the wavelength of X-rays, θ is the scattering angle between the incident beam and the scattered radiation, and r is the distance between the two scattering centers within the particle.

$p(r)$ was evaluated from the measured $I(q)$ using the Indirect Fourier Transformation Method (program IFT)[22,23] and its extension Generalized Indirect Fourier transformation method GIFT.[24,25,26,27]

IFT as a completely model-free method which can only be applied for the "dilute" systems where interparticle interactions can be neglected. At higher concentrations of scattering particles interparticle correlations strongly affect the scattering intensity $I(q)$ and must be taken into account during the evaluation procedure using recently developed GIFT technique.

GIFT is based on the assumption that the scattering intensity $I(q)$ can be represented as a product of the intraparticle scattering contribution $P(q)$ (form factor) with $p(r)$ as its Fourier transformation and the interparticle scattering contribution $S(q)$ (structure factor) describing the interparticle interactions in reciprocal (q) space:

$$I(q) = nP(q)S(q) \qquad (3)$$

where n is the number density of particles. $P(q)$ represents the scattering of a free particle that is given by Eq. 2. In real (r) space the interparticle interactions are described by the total correlation function $h(r)=g(r)-1$, with $g(r)$ being the radial distribution function and r the distance between the centers of two particles.[28] Since the connection between the functions from q and r space is a Fourier transformation, $S(q)$ and $h(r)$, similarly as $P(q)$ and $p(r)$, form another Fourier transform pair:[28]

$$S(q) = 1 + 4\pi n\int_0^\infty h(r)r^2\frac{\sin(qr)}{qr}dr \qquad (4)$$

Equation 3 is exact only in the case of monodisperse isotropic dispersions of spherical particles. However, it has been shown with many examples that by introducing the "averaged structure factor", $S_{ave}(q)$, or more exact "effective structure factor", $S_{eff}(q)$, one can obtain good results also for polydisperse spheres or cylinders[26] and even for inhomogeneous particles.[24,25,29,30]

The GIFT evaluation technique simultaneously determines the $P(q)$ that remains model-free, and $S(q)$, which has to be calculated according to the model for interparticle interactions by finding the global mean deviation minimum.[27] In the present work, a polydisperse system of hard spheres is chosen as a model, and a Percus-Yevick approximation is used as a method for the calculation of $S(q)$. The resulting averaged structure factor, with

average taken over the weight contributions of partial structure factors for individual monodisperse systems, $S_{ave}(q)$, is described by three parameters: the volume fraction ϕ, the interaction radius R and the polydispersity μ.

In the case of spherical symmetry $p(r)$ simplifies into: $p(r) = r^2\Delta\tilde{\rho}^2(r)$[31,32] where $\Delta\tilde{\rho}^2(r)$ is the spatial averaged autocorrelation function (convolution square) of the electron density fluctuations given by the general expression[32]

$$\Delta\tilde{\rho}^2(r) = \left\langle \Delta\tilde{\rho}^2(\boldsymbol{r}) \right\rangle = \left\langle \int_{-\infty}^{+\infty} \Delta\rho(\boldsymbol{r}_1)\Delta\rho(\boldsymbol{r}_1 - \boldsymbol{r})d\boldsymbol{r}_1 \right\rangle \qquad (5)$$

in which $\Delta\rho(\boldsymbol{r})$ represents the local scattering contrast, that is the difference between the local scattering particle's electron density $\rho(\boldsymbol{r})$ and the average electron density of the sample $\bar{\rho}$. The scattering contrast profile $\Delta\rho(\boldsymbol{r})$ of the scattering particles that provides valuable information on the internal structure of scattering particles can be calculated from $p(r)$ function by a convolution square root operation utilizing the DECON program.[33,34,35,36]

3. Results and Discussion

In the Figure 1 the experimental scattering curves (symbols) of the Tween 40® aqueous solutions at various surfactant concentrations are shown after subtraction of solvent scattering in a plot of intensity versus scattering vector q.

Figure 1a shows the SAXS spectra with the lines representing a fit to the experimental data as obtained by the indirect Fourier transformation method IFT method for the solutions with lower concentration of surfactant (w = 0.01 and 0.025) and by the generalized indirect transformation method GIFT for all other solutions. The results of the IFT procedure are the pair-distance distribution functions $p(r)$, whereas at the GIFT procedure also the structure factors $S_{ave}(q)$ are obtained. They are shown in Figures 2b and 3b and discussed in more details below.

As seen in Figure 1a the overall scattering intensity is increasing with the increasing surfactant concentration related to the growing number of particles in the scattering volume. In parallel, the inner central peak (at low q values) is gradually disappearing, indicating the increasing role of interparticle interactions.

In Figure 1b the SAXS curves are normalized to the unit surfactant concentration and the effect of increasing intensity with growing number of particles is eliminated (see Eq. 3). Evidently, the height of the central peak and the intensity at low q regime, respectively, are decreasing with increasing surfactant concentration. This is a characteristic of the dominating repulsive (liquid-type) interactions among the scattering particles. The side maximum (at approximately $q = 1$ nm^{-1}), which is related to the particle form factor, stays at the approximately same position. Assuming that the shape of the particles remains the same upon change in the concentration, nearly constant particle dimensions are expected.

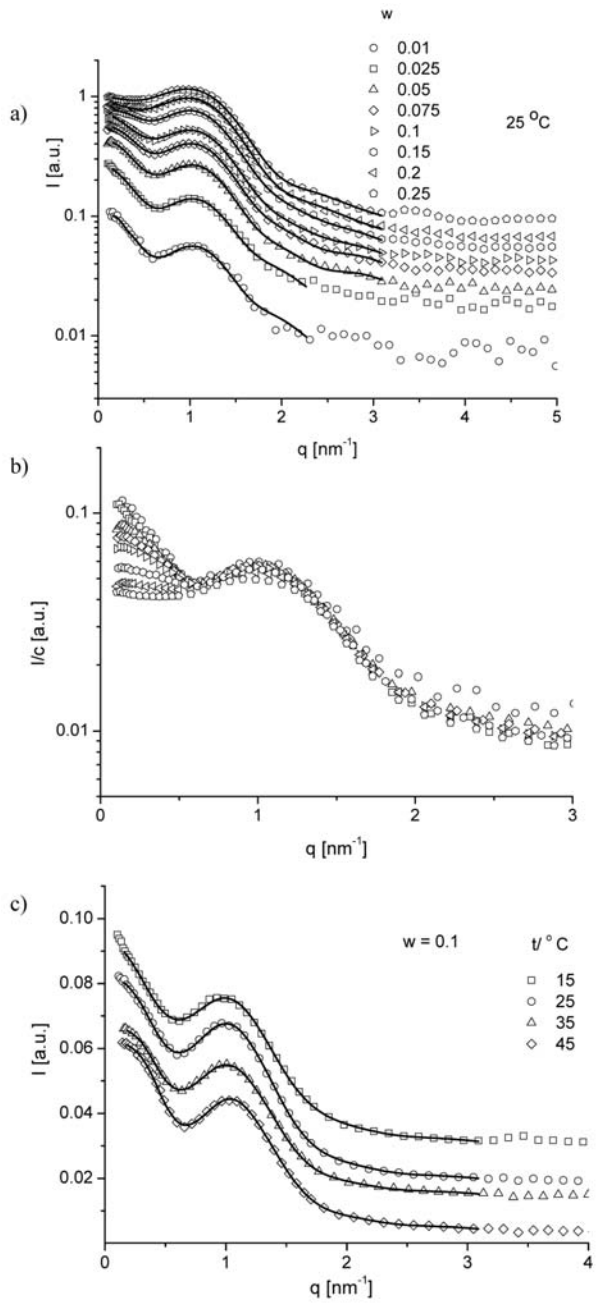

Figure 1.

a) Experimental SAXS spectra of Tween 40® aqueous solutions with different surfactant concentrations at 25 °C (symbols). w = weight fraction of the surfactant in the solution. Lines represent the IFT (w = 0.01 and 0.025) and GIFT fits (w ≥ 0.05) to the experimental data.

b) The same SAXS spectra but normalized to unit surfactant concentrations.

c) Temperature dependent experimental SAXS spectra of Tween 40® aqueous solutions with the weight fraction of surfactant, w = 0.1. The curves were shifted for the sake of clarity. Lines represent the GIFT fits to the experimental data.

As shown in Figure 1c, the general shape of the scattering curves for Tween® micellar aqueous solutions remains almost unaltered for all temperatures considered at constant composition: the position of the side maximum is constant indicating that the dimensions of the particles are not affected by the temperature considerably. A slight difference can be observed at low *q* regime of the scattering curves, reflecting the interparticle interference.

Essential information on the particle geometry can be obtained from the pair distance distribution function *p(r).* Experimental SAXS spectra of Tween 40® aqueous solutions (Figure 1) were evaluated utilizing the IFT and GIFT methods. The resulting *p(r)* functions and the corresponding structure factors $S_{ave}(q)$ are presented in Figures 2a and 2b.

The shape of the *p(r)* functions is characteristic for the heterogenous spherical micelles with the difference in the core and the shell scattering contrast.[25,29] It could be seen that *p(r)* curves are not symmetric at higher concentrations, which would suggest the presence of non-spherical aggregates or elongation. Interpreted as such also relatively high values of polydispersity at w = 0. 15 and 0.2, resulting from the fitting procedure to the hard sphere model for structure factor, seem reasonable.

One can estimate the maximal distance D_{max} within one particle from the abscissa value where *p(r)* function vanishes.

The corresponding structure factors are presented in Figure 2b. The $S_{ave}(0)$ value decreases considerably with increasing concentration indicating the increasing volume fraction of the scatttering particles. At the same time the interaction peak becomes sharper and moves toward higher *q* values, reflecting the decreasing mean distance between neighboring particles.

The distribution of the electron density contrast within the Tween 40® micelles resulting from the deconvolution[33,34,35,36] of the corresponding *p(r)* function presented in Figure 2c shows two regions of opposite sign. By taking into account the molar volumes of the 5-membered ring and oxyethylene chains, the electron density of the polar part of the Tween 40® molecule can be estimated to be approximately 424 $e^- nm^{-3.}$ The corresponding electron densities of the nonpolar part (C_{15}) and pure water are 298 and 334 $e^- nm^{-3}$, respectively, which means that the the C_{15} hydrophobic core has a negative and the polar shell a positive scattering contrast against water.

Furthermore, these estimations suggest higher values of the positive scattering contrast than those observed experimentally (Figure 2c). Since the hydrated water may substantially decrease the average electron density of the polar shell, the observed deviation may be ascribed to a strong hydration of the oxyethylene chains in the shell of the micelles. Similar behavior has been observed at some poly(ethylene glycol) monooctyl ethers (C_8E_j)[39] and Brij 35[29,30] in aqueous solutions.

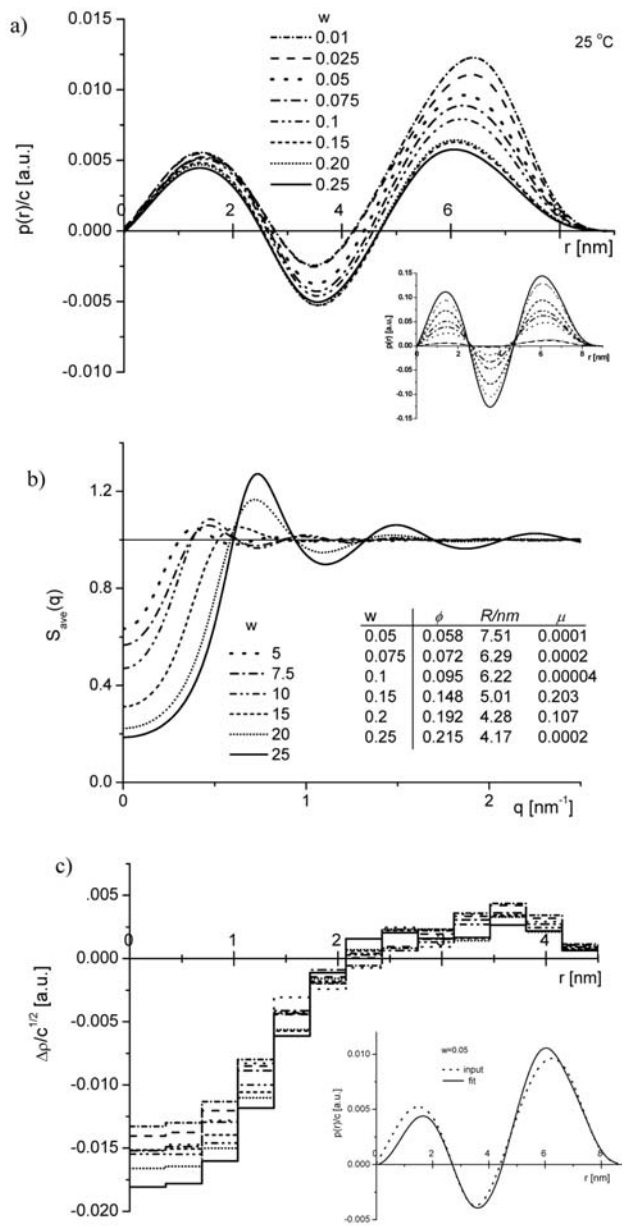

Figure 2. The results of the IFT (w = 0.01 and 0.025) and GIFT (w ≥ 0.05) evaluation of the scattering curves from Figures 1a and 1b together with the corresponding electron density contrast profiles at 25 °C.

a) Pair-distance distribution functions normalized to unit surfactant concentration. Inset: the same functions but without normalization.

b) Averaged structure factors $S_{ave}(q)$. Inset: parameters of the modeled $S_{ave}(q)$, volume fraction ϕ, interaction radius R, and polydispersity μ.

c) Electron density contrast profiles Δρ(r) of Tween 40® micelles in aqueous solutions, normalized by the square root of surfactant concentration.

Inset: An example of the comparison between input p(r) and its approximation as obtained by the convolution square root operation.

The radius of the hydrophobic core can be estimated from the abscissa value where the scattering contrast

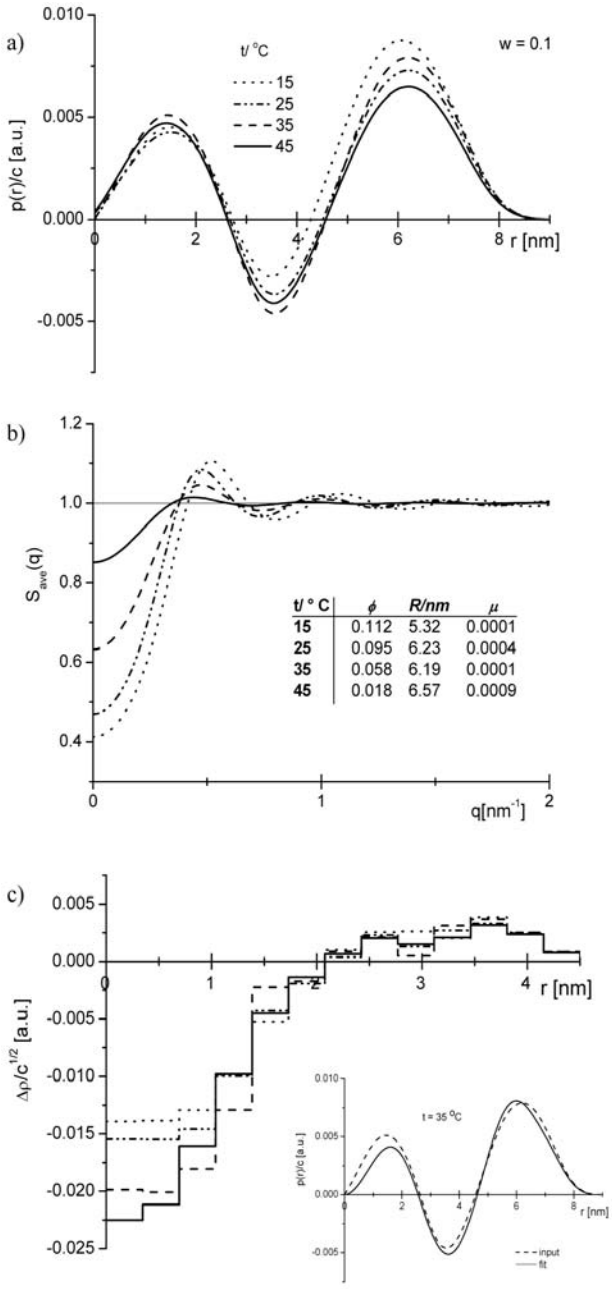

Figure 3. The results of the GIFT evaluation of the scattering curves from Figures 1c and corresponding electron density contrast profiles.

a) Pair-distance distribution functions normalized to unit surfactant concentration.

b) Averaged structure factors $S_{ave}(q)$. Inset: parameters of the modeled $S_{ave}(q)$, volume fraction ϕ, interaction radius R, and polydispersity μ.

c) Temperature dependence of the electron density contrast profiles Δρ(r) of Tween 40® micelles in aqueous solutions. Inset: An example of the comparison between input p(r) and its approximation as obtained by the convolution square root operation.

changes sign (Figure 2c). Estimates of the Tween 40® micelle hard-core radii were obtained from the intersection of these profiles with the abscissa at $r \approx 2.4$ nm (w = 0.01 and 0.025) and $r \approx 2.1$ at higher concentrations. The obtained values are in reasonable agreement with the theoretically calculated length of the fully stretched C_{15} chain (= 1.92 nm)[40] and the unhydrated radius for the Tween 40® micelles, obtained from density measurements (= 2.51 nm).[14]

In the literature the micellar aggregation number, N = 91 ± 1, obtained from the fluorescence study at 25 °C for Tween 40® is reported.[41] Assuming that the micelles are spheres, the aggregation number can be calculated from the molar volume of the lipophilic part of surfactant ($V(-CH_3) = 19.2$ cm^3 mol^{-1}, $V(-CH_{2-}) = 16.1$ cm^3 mol^{-1})[37,38] and the volume of the micellar core. For $r = 2.1$ nm the aggregation number N ≈ 95 could be estimated, which is in good agreement with the reported value.

Next, the effect of the temperature on the micellar properties of aqueous solutions was investigated. The pair-distance distribution functions *p(r)* and structure factors $S_{ave}(q)$ in Tween 40® aqueous solution (w = 0.1), obtained from experimental SAXS spectra (Figure 1 c) are presented in Figure 3.

As shown in Figure 3a, the qualitative shape of the pair-distance distribution function, *p(r)*, i.e., the shape of the Tween 40® particles formed in the solution, does not change significantly upon varying the solution composition or temperature.

The variation of the excess density profile with temperature is shown in Figure 3c. Since the input pair-distance distribution functions do not differ significantly, the resulting excess electron density profiles have the same shape at all measured temperatures. Due to the dehydration of ethylene oxide chains, a change in the electron density with the temperature is to be expected, but this anticipation is not confirmed. Moreover, the intercepts of the contrast profiles coincide perfectly at $r \approx 2.1$ nm, confirming that the temperature does not affect the shape and size of the Tween 40® micelles in aqueous solutions substantially.

Similar behaviour was observed at some other polyoxyethlyene surfactants (C_8E_j) aqueous solutions.[39]

The corresponding structure factors are presented in Figure 3b. The $S_{ave}(0)$ value decreases with decreasing temperature, at the same time the interaction peak becomes slightly sharper at lower temperatures, but moves hardly to higher *q* values. As anticipated in the presence of a repulsive interaction, the compressibility (reflected in $S_{ave}(0)$) dimnishes. Evidently the repulsive interactions are stronger at lower temperatures.

In Figure 5 concentration dependence of the volume fraction of the scattering particles, ϕ, and interaction radius, *R*, as derived from the structure factors are presented at all investigated temperatures.

At lower temperatures (15, 25 °C), the effective volume fractions, ϕ, are very close to the weight fractions of disperse phase (surfactant weight fractions in the solution), and they are lower at higher temperatures (35,

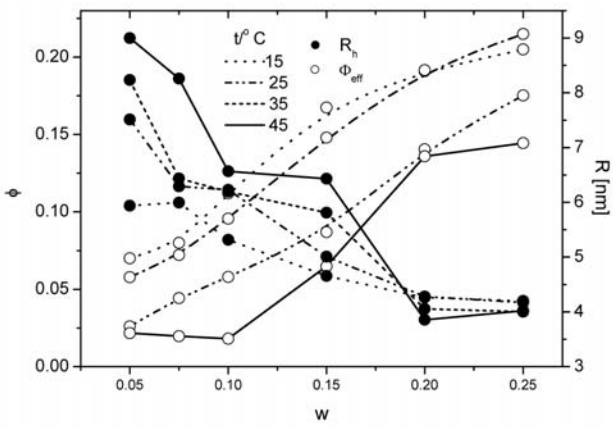

Figure 4. The structural parameters, effective volume, ϕ, and the interaction radius, R, for the averaged Percus-Yevick structure factor $S_{ave}(q)$ of Tween 40® in aqueous solutions as a function of concentration of surfactant and temperature. The connecting lines are shown as guides to the eye.

45 °C). This indicates a weak hydration of the micelles, although from the electron density a strong hydration of polyoxyethylene parts (Scheme 1) is evident. It could be assumed that the polar chains are hydrated and folded tightly in the polar shell of the micelles. Presumably the polyoxyethylene chains are linked together via hydrogen bonds forming a compacter structure as observed at some other polyoxyethylene surfactants (C_8E_j, Brij 35),[29,39] possessing only one polyoxyethylene chain. While at C_8E_j[39] and Brij 35[29] aqueous solutions the vanishing point of the corresponding contrasts in the electronic density could not be read distinctively due to the strong hydration shell of micelles,[29,39] no evidence for a strong hydration for Tween 40® micelles in the aqueous solution was found.

It is known, that the hydration is weaker at higher temperatures resulting presumably in lower values of the effective volume fraction, ϕ.

The effective interaction radius, R, is the half of the center-to-center distance between two micelles at closest approach. In our case, at lower concetrations R appears to be much larger than half the maximum dimensions from the pair-distance distribution functions. Upon increasing concentration R decreases and at w > 0.15 the interaction radii are very close to the values obtained from the pair-distribution functions at all investigated temperatures.

Large R values do not necessarily indicate large micelles; they rather suggest long range interactions resulting from i.e. hydration shells. It could be concluded that at lower concentrations these long range interactions are more pronounced. Somehow this finding is in agreement with the larger radii of the no-polar core of the micelles estimated for the solutions with w = 0.01 and 0.025. At lower concentrations the surfactant molecules associate in the micelles but the packing obviously is still rather loose. The hydrated polyoxyethylene chains presumably are not packed very close yet and some could penetrate into the surrounding continuous phase resulting in the long range interactions.

The effective interaction radius, R, is decreasing as the fraction of the disperse phase is growing at all temperatures. At w = 0.25 its values agrees well with the half the maximum dimensions from the pair-distance distribution functions. It could be assumed, that at higher concentrations the polyoxyethylene chains are folded more tightly in the polar micelle shell. Thus less polar tails are embedded in the surrounding water and the long range interactions are less pronounced.

At the same time the effective volume fractions are increasing in accordance with the weight fraction of the surfactant in the solution. It is known that hydrated water has a considerable influence (increase) on the effective micellar volume fraction and the resulting decreased osmotic compressibility of the system, manifested by a decreased $S_{ave}(0)$ value. However, a table shown as an inset of the Figure 2b indicates that estimated volume fraction by GIFT can be accounted for by intrinsic volume of surfactant only, as if a micelle is in a 'dry' state at room temperature. Supposing that these results of the GIFT analysis have a physical meaning, this might indicate a compensation between an increased excluded volume by hydrated water and a weak intermicellar adhesive (attractive) interaction that may be specific to Tween 40, although in general, it is known that poly(ethylene glycol) based surfactants show a nearly hard sphere interaction. A strongly reduced effective volume (less than 0.02 at 45 °C) is too small for the experimental 10% surfactant weight fraction and this discrepancy could not be attributed solely to dehydration. Because no diminishing forward intensity at high temperature was observed an induced attractive interaction related to critical phenomena in the solutions at higer temperatures could be assumed.

4. Conclusions

In this paper we reported small-angle X-ray scattering (SAXS) study of the surfactant Tween 40® in aqueous solutions in the temperature range between 15 and 45 °C. The experimental SAXS data were evaluated using indirect Fourier transformation method, IFT, and the generalized indirect Fourier transformation method, GIFT method. The first one (model free) was applied analyzing the SAXS data of diluted solutions, whereas the GIFT method made possible the evaluation of the data in concentrated systems with interacting scattering parameters. In this way, the size and shape of interacting scattering particles in real space were deduced.

In the Tween 40® aqueous solutions (surfactant concentrations from 1 to 25 weight %) globular micelles with maximal distance D_{max} within one particle at about 9 nm were found.

At higher concentrations the formation of non spherical or elongated aggregates also could be assumed.

The shape and the size of the micelles show no explicit temperature dependence. At low concentrations slightly larger radii of the hydrophobic core around 2.4 nm were found indicating the looser formation of the micelles in diluted solutions. The radii of the hydrophobic core at higher concentrations are about 2.1 nm.

The parameters of the averaged structure parameters $S_{ave}(q)$, the volume fraction of the scattering particles, ϕ, and interaction radius, R, indicating a rather weak micelle hydration shell, that is even lessen with the increasing temperature.

5. Acknowledgements

This work was supported by the Ministry of Higher Education, Science and Technology and by the Agency for Research of Republic of Slovenia through the Grants No. P1-0201 and J1-6653. The author would like to express her gratitude to the Alexander von Humboldt Foundation, Germany, for the donation of the small angle X-ray scattering system and to Mr. Tone Kokalj for performing SAXS measurements.

6. References

1. N. Garti, A. Spernath, A. Aserin, R. Lutz, *Soft Matter* **2005**, *1*, 206–218.
2. P. P. Constanitinides, J. P. Scarlat, *Int. J. Pharm.* **1997**, *158*, 57–68.
3. S. S. Prichanont, D.J. Leak, D.C. Stuckey, *Colloid Surf. A* **2000**, 166, 177–186.
4. K.-M. Park, C.-K. Kim, *Int. J. Pharm*. **1999**, *181*, 173–179.
5. A. Radomska, R. Dobrucki, *Int. J. Pharm.* **2000,** *196*, 131–134.
6. L. de Campo, A. Yaghmur, N. Gart, M. E. Leser, B. Folmer, O. Glatter, *J. Colloid Interface Sci.* **2004**, *274*, 251–267.
7. A. Yaghmur, L. De Campo, A. Aserin, N. Garti, O. Glatter, *Phys. Chem. Chem. Phys.* **2004**, *6*, 1524–1533.
8. F. Podlogar, M. Gašperlin, M. Tomšič, A. Jamnik, M. Bešter-Rogač, *Int. J. Pharm* **2004**, *276*, 115–128
9. F. Podlogar, M. Bešter-Rogač, M. Gašperlin, *Int. J. Pharm* **2005**, *302*, 68–77.
10. M. Tomšič, F. Podlogar, M. Gašperlin, M. Bešter-Rogač, A. Jamnik, A., *Int. J. Pharm* **2006**, *327,* 170–177.
11. P. Thanasukarn, R. Pongsawatmanit. D. J. McClements, *J. Agric. Food. Chem.* **2006**, *54*. 3591–3597.
12. http://www.foodstandards.gov.uk/safereating/chemsafe/additivesbranch/enumberlist (viewed last May 15 2007).
13. S. K. Hait, S. P. Moulik, *J. Sufactants Deterg.* **2001**, *4/3*, 303–309.
14. K. M. Glenn, S. Moroze, R. M. Palepu, S. C. Bhattacharya, *J. Disper. Sci. Technol.* **2005**, *26,* 79–86.
15. C. Carnero Ruiz, J. A. Molina-Bolivar, J. Aguiar, G. MacIsaac, S. Moroze, R. Palepu, *Colloid Polym. Sci.* **2003**, *281*, 531–54.
16. R. Mahajan, J. Chawla, M. Bakshi, G. Kaur, V. Aswal, P. Goyal, *Colloid Polym Sci.* **2004**, *283*, 164–168
17. S. Ghosh, *J. Colloid Interface Sci*. **2001**, *244*, 128–138.
18. Y. R. Suradkar, S. S. Bhagwat, *J. Chem. Eng. Data* **2006**, *51*, 2026–2031.
19. R. Mahajan, J. Chawla, M. Bakshi, *Colloid Polym. Sci.* **2004**, *282*, 1165–1168.
20. H. Stabinger, O. Kratky, *Makromol. Chem.* **1978**, *179*, 1655–1659.
21. O. Glatter, *J. Appl. Crystallogr.* **1979**, *12*, 166–175.
22. O. Glatter, *Acta Phys. Austriaca* **1977**, *47*, 83–102.
23. O. Glatter, *J. Appl. Crystallogr.* **1977**, *10*, 415–421.
24. J. Brunner-Popela, O. Glatter, *J. Appl. Crystallogr*. **1997**, *30*, 431–442.
25. B. Weyerich, J. Brunner-Popela, O. Glatter, *J. Appl. Crystallogr.* **1999**, *32*, 197–209.
26. J. Brunner-Popela, R. Mittelbach, R. Strey, K.V. Schubert, E. W. Kaler, O. Glatter, *J. Chem. Phys.* **1999**, *21*, 10623–10632.
27. A. Bergmann, G. Fritz, O. Glatter, *J. Appl. Crystallogr*. **2000**, *33*, 1212–1216.
28. J. P. Hansen, I.R. McDonald, In: *The Theory of Simple Liquids;* Academic: London, **1990**.
29. M. Tomšič, M. Bešter-Rogač, A. Jamnik, W. Kunz, D. Touraud, A. Bergmann, O. Glatter, *J. Phys. Chem. B* **2004**, *108*, 7021–7032.
30. M. Tomšič, M. Bešter-Rogač, A. Jamnik, W. Kunz, D. Touraud, A. Bergmann, O. Glatter, *J. Colloid Interface Sci.* **2006**, *294*, 194–211.
31. O. Glatter, Interpretation. in: O. Glatter, O. Kratky (Eds): Small Angle X-ray Scattering, Academic Press Inc. London Ltd.: London **1983**.
32. O. Glatter, The Inverse Scattering Problem in Small Angle X-ray Scattering. in: Lindner, P., Zemb, T. (Eds): Neutron, X-rays and Light: Scattering Methods Applied to Soft Condensed Matter, Elsevier:North-Holland, Amsterdam **2002.**
33. O. Glatter, Fourier Transformation and Deconvolution. in: Lindner, P., Zemb, T. (Eds.): Neutron, X-rays and Light: Scattering Methods Applied to Soft Condensed Matter,; Elsevier: North-Holland, Amsterdam **2002**.
34. O. Glatter, *J. Appl. Crystallogr.* **1981,** *14*, 101–108.
35. O. Glatter, B. Hainisch, *J. Appl. Crystallogr.* **1984,** *17*, 435–441.
36. R. Mittelbach, O. Glatter, *J. Appl. Crystallogr.* **1998**, *31*, 600–608.
37. H. Durchschlag, P. Zipper*, Prog. Colloid Polym. Sci*. **1994**, *94*, 20–39.
38. H. Durchschlag, P. Zipper, *Jorn. Com. Esp. Deterg*. **1995**, *26*, 275–292.
39. J. Lah, M. Bešter-Rogač, T.-M. Perger, G. Vesnaver, *J. Phys. Chem. B* **2006**, *110*, 23279–23291.
40. C. Tanford, *J. Phys. Chem.* **1972**, *76*, 3020–3024.
41. G. B. Behera, B. K. Mishra, P.K. Behera, M. Panda, *Adv. Colloid Interface Sci.* **1999**, *82*, 1–42.

Povzetek

Z metodo ozkokotnega rentgenskega sipanja smo raziskovali strukturne lastnosti neionskega surfaktanta polioksietilen sorbitan monopalmitata ($C_{62}H_{122}O_{26}$, komercialno ime Tween 40® ali Polysorbat 40) v vodnih raztopinah v temperaturnem območju med 15 in 45 °C. Eksperimentalne krivulje rentgenskega sipanja smo za razredčene raztopine ovrednotiili z metodo indirektne Fourierovo transformacije (IFT). Pri višjih koncentracijah pa smo uporabili posplošeno (generalizirano) indirektno Fourierovo transformacijo. (GIFT), ki je osnovana na simultani določitvi intra- in itermolekularnega prispevka k celotnemu sipanju. Ugotovili smo, da Tween 40® v vodnih raztopinah tvori globularne micele tipa hidrofobno jedro-hidrofilna lupina z maksimalno dimenzijo 9 nm in radijem hidrofobnega jedra 2.1–2.4 nm. Velikost in oblika micel se bistveno ne spreminja s temperaturo, pri višjih koncentracijah pa je možno predvideti tudi pojav nesferičnih ali podolgovatih agregatov.